

Exploratory Spectroscopy of Magnetic Cataclysmic Variables Candidates and Other Variable Objects

A. S. Oliveira

IP&D, Universidade do Vale do Paraíba, 12244-000, São José dos Campos, SP, Brazil
alexandre@univap.br

C. V. Rodrigues, D. Cieslinski, F. J. Jablonski

Divisão de Astrofísica, Instituto Nacional de Pesquisas Espaciais, 12227-010, São José dos Campos, SP, Brazil

K. M. G. Silva

Gemini Observatory, Casilla 603, La Serena, Chile

L. A. Almeida

Instituto de Astronomia, Geofísica e Ciências Atmosféricas, Universidade de São Paulo, 05508-900, São Paulo, SP, Brazil

A. Rodríguez-Ardila

Laboratório Nacional de Astrofísica LNA/MCTI, 37504-364, Itajubá MG, Brazil
and

M. S. Palhares

IP&D, Universidade do Vale do Paraíba, 12244-000, São José dos Campos, SP, Brazil

ABSTRACT

The increasing number of synoptic surveys made by small robotic telescopes, as the photometric Catalina Real-Time Transient Survey (CRTS), represents a unique opportunity for the discovery of new variable objects, improving the samples of many classes of variables. Our goal is the discovery of new magnetic Cataclysmic Variables (mCVs). They are rare objects, which probe interesting accretion scenarios controlled by the white-dwarf magnetic field. We performed an optical spectroscopic survey to search for signatures of magnetic accretion on 47 variable objects selected mostly from CRTS. Our sample includes 13 polar strong candidates, from which 5 are new discoveries. Accretion disks seem to be present in other 19 objects. One is a previously known probable intermediate polar. We suggest 8 other objects could also be of this class. In particular, 7 of them have spectra consistent with short-period intermediate polars. We suggest one object is a novalike of the VY Scl class. We also caught one dwarf nova in eruption and confirmed a Nova discovered in X-rays. Follow-up observations are necessary to confirm the classification of some mCVs. Our sample also includes 8 stars in the horizontal or asymptotic giant branches: 2 known RR Lyrae stars, 3 new RR Lyrae, 2 new pulsating red giants and a new Mira. We estimated the period for 5 of them. We report the detection of 7 extragalactic sources, 5 of them classified as AGNs. Some of these sources display large variability amplitudes consistent with the possibility of harboring an optically violently variable (OVV) quasar.

Subject headings: galaxies: active — novae, cataclysmic variables — stars: dwarf novae — stars: oscillations — stars: variables: general — techniques: spectroscopic

1. INTRODUCTION

Cataclysmic Variable stars (CVs) are binary systems composed of a white dwarf accreting mass from a less massive main sequence companion star via Roche lobe overflow (e.g., Warner 1995). The mass transfer in these systems leads to a decrease of the orbital period and demands a loss of orbital angular momentum that is usually attributed to two complementary mechanisms: the magnetic braking of the secondary star in longer orbital period systems and the gravitational radiation in shorter period systems, in which the former mechanism is less efficient. The accretion of the transferred material on the white dwarf occurs by the formation of an accretion disk, which is the dominant source of radiation in the binary system. The accretion disk may suffer recurrent episodes of instability known as Dwarf Nova outbursts that increases the luminosity of the system by 2 – 6 magnitudes in timescales as short as one day.

If the white dwarf has a strong enough magnetic field, however, the transferred ionized material connects to the magnetic field lines and accretes directly to the white dwarf surface, close to the magnetic poles, via an accretion column instead of a disk. These systems are known as magnetic Cataclysmic Variables (mCVs) and can be classified either as polars, whose magnetic fields are more intense ($B \sim 7 - 230$ MG), or as intermediate polars (IPs), in which $B \sim 1 - 10$ MG. The distinctive characteristic of the polars is the synchronization of the white-dwarf spin and the orbital period, caused by magnetic locking of the primary and secondary stars (see Cropper 1990, for a review on polars). The matter falling through the accretion column emits cyclotron radiation, which is highly polarized and anisotropic and that dominates the optical and infrared emission. Polars alternate between high and low brightness states in optical and X-rays with drops of 1 – 3 magnitudes, probably associated to variations in the mass transfer rate. The optical spectrum of polars displays high ionization emission lines of He II, the C III/N III blend at 4650 Å and Balmer lines. When in low state, the optical spectrum may show cyclotron humps. Intermediate polars, on the other hand, are not synchronized systems, and the distinct spin and orbital periods manifest in optical and X-ray variability. IPs may present

an accretion disk, truncated in its inner region by the magnetosphere of the white dwarf. The optical spectra of IPs may be quite similar to the spectra of polars, although He II 4686 Å is generally slightly weaker relative to H β in IPs than in polars. However, non-magnetic CVs can also present the He II 4686 Å emission line, making difficult to distinguish spectra of IPs and dwarf novae. Magnetic CVs have mostly been discovered by X-ray all-sky surveys, as polars usually are intense soft X-ray sources while IPs emits predominantly in hard X-rays.

A large number of new CV systems has been discovered (Szkody et al. 2011) by surveys based on color selection, like SDSS (York et al. 2000). Surveys based on variability are also prolific in finding new CVs and, in the near future, the Large Synoptic Survey Telescope - LSST - is expected to strongly impact the statistic of CVs. One of these variability surveys is the Catalina Real-Time Transient Survey - CRTS (Drake et al. 2009, 2014). The CRTS combines three distinct surveys - the Mount Lemmon Survey (MLS) and the Catalina Schmidt Survey (CSS) in the northern hemisphere and the Siding Spring Survey (SSS) in the south - that monitor an area of 30 000 deg² with a typical cadence of two weeks, reaching a depth of 19-21 magnitudes. The CRTS has already found thousands of CV candidates that are rapidly published in their website¹ and are subject to follow-up investigation (e.g., Coppejans et al. 2014; Drake et al. 2014; Breedt et al. 2014; Thorstensen & Skinner 2012; Coppejans et al. 2016). As the early CRTS criterion for detecting transients was the brightening by 2 or more magnitudes, it turns out that it is very effective in discovering new dwarf novae, as these follow-up works have shown.

In this work we are interested in finding new mCVs in order to increase the number of known members of this class. An increased statistics would help to unveil issues concerning, for instance, the evolution scenario of mCVs, specially the possible evolutionary relation between IPs and polars. We selected a sample of 47 variable objects, mainly from the CRTS catalogue in which case we tried to choose light curves that resemble the photometric behavior of mCVs, as variation

¹<http://crtst.catalogue>

between high and low brightness states. We also included in our sample mCVs candidates without previous spectroscopic measurements. Previous reports of X-ray detections and VSNET and ATel alerts were considered. Besides, objects should have suitable apparent magnitudes and coordinates for SOAR observations. For the selected sample, we obtained exploratory spectra aiming to identify spectral features that could be signatures of high-ionization mass accretion representative of mCVs.

This article is organized as follows. In Section 2, we describe our spectroscopic observations. The adopted procedure for the temporal analysis of CRTS photometric data is presented in Section 3. Our spectroscopic results and the proposed classification for each object are shown in Section 4, while some discussion and a summary of our results are presented in the last section.

2. OBSERVATIONS

The exploratory spectra were obtained using SOAR 4.1 m telescope, on Cerro Pachón, Chile, and the Perkin & Elmer 1.6 m telescope at Observatório do Pico dos Dias (OPD-LNA/MCTI), located in the southeast of Brazil. The RA ordered list of observed objects is shown in Table 1. The identification of the objects from the CRTS is of the form TTTyyymmdd:hhmmss \pm ddmmss, where TTT indicates one of the three dedicated telescopes of the survey – CSS, SSS or MLS – yymmdd is the discovery date of the transient and hhmmss \pm ddmmss are the target coordinates. In order to avoid confusion between transients discovered by the same telescope at the same date, and for simplicity, we will abbreviate these IDs as TTThhmm \pm dd.

The SOAR Telescope was operated in service mode and the spectra were obtained using the Goodman High Throughput Spectrograph (Clemens et al. 2004), which employs Volume Phase Holographic (VPH) gratings to maximize throughput, reaching down to the atmospheric cutoff at 3200 Å. It is equipped with a Fairchild 4096 \times 4096 CCD with 15 micron pixel $^{-1}$. The spectrograph was set to operate with the 600 1 mm $^{-1}$ grating, 1.68" slit, and the GG 385 blocking filter, yielding a spectral resolution of 7 Å FWHM in the range from 4350 to 7005 Å. Three

exposures of each scientific target were obtained to remove cosmic rays. CuHeAr lamp exposures were used for wavelength calibration, which resulted in typical 0.8 Å or about 45 km s $^{-1}$ calibration RMS residuals. The [O I] 5577, 6300 and 6363 Å telluric spectral lines were used to assess the calibration accuracy. The slit was aligned to the parallactic angle to avoid light losses due to the atmospheric differential refraction. Bias images and quartz lamps calibration flats were taken to correct for the detector read-out noise and sensitivity. Spectra of spectrophotometric standards (Hamuy et al. 1992) were used for flux calibration. The data reduction, spectra extraction and calibrations were performed using IRAF² standard routines.

The OPD-LNA observations were carried out using a Boller & Chivens Cassegrain spectrograph on March and September of 2012. A 300 1 mm $^{-1}$ grating, blazed in 6400 Å, was used in these two missions, providing a spectral coverage from 4100 to 8530 Å. The slit aperture was set in 2.50" in March and 2.00" in September, giving a spectral resolution of 7 Å and 6 Å (FWHM), respectively. Two different thin, back-illuminated CCD detectors were used: an iKon-L936-BV (March) and an iKon-L936-BR-DD (September), both with 2048 \times 2048 pixels and 13.5 \times 13.5 micron pixel $^{-1}$. In the March mission, the GG 385 blocking filter was used, while in September no filter was necessary. All targets were observed with integration times of 600 or 900 s. Multiple exposures (normally 2 or 3) were done aiming to improve the S/N ratio and to minimize effects of cosmic rays in the images. HeAr comparison lamp exposures were obtained after each target observation for wavelength calibration. For flux calibration, we observed the spectrophotometric standard stars HR 3454 and HR 9087 from Hamuy et al. (1992). In all nights, images of dome flats and bias were also obtained. Corrections for bias and flatfield, extraction of the spectra, wavelength calibration and extinction and flux calibrations were carried out using IRAF standard routines.

²IRAF is distributed by the National Optical Astronomy Observatories, which are operated by the Association of Universities for Research in Astronomy, Inc., under cooperative agreement with the National Science Foundation.

TABLE 1
LIST OF OBSERVED TARGETS.

Object name	Abbreviation	RA (J2000)	Dec (J2000)	Date obs.	Telesc.	Exp. time (s)	Type ^a
CSS091009:010412-031341	CSS0104-03	01:04:12	-03:13:41	2012 Aug 25	SOAR	3600	D/IP
MLS110207:014023+020639	MLS0140+02	01:40:23	+02:06:39	2012 Aug 25	SOAR	900	RRL
CSS091215:021311+002153	CSS0213+00	02:13:11	+00:21:53	2012 Sep 09	SOAR	8100	E
MLS110213:022733+130617	MLS0227+13	02:27:33	+13:06:17	2012 Sep 09	SOAR	3600	P
CSS071206:031525-014051	CSS0315-01	03:15:25	-01:40:51	2012 Nov 13	SOAR	8100	E
CSS090922:032603+252534	CSS0326+25	03:26:03	+25:25:34	2012 Nov 20	SOAR	3600	D
CSS091109:035759+102943	CSS0357+10	03:57:59	+10:29:43	2012 Nov 12	SOAR	8100	P
MLS101203:045625+182634	MLS0456+18	04:56:25	+18:26:34	2012 Nov 13	SOAR	8100	P
XMM-MSL J063045.9-603110	XMM0630-60	06:30:45	-60:31:13	2012 Nov 12	SOAR	8100	N
MLS101226:072033+172437	MLS0720+17	07:20:33	+17:24:37	2012 Nov 12	SOAR	1440	P
1RXS J072103.3-055854	1RXS0721-05	07:21:03	-05:59:20	2012 May 01	SOAR	1440	HA
MLS120127:085402+133633	MLS0854+13	08:54:02	+13:36:33	2012 Dec 15	SOAR	8100	P
MLS110210:100054+065557	MLS1000+06	10:00:54	+06:55:57	2012 Mar 26	OPD	2700	RRL
1RXS J100211.4-192534	1RXS1002-19	10:02:11	-19:25:36	2012 May 30	SOAR	360	P
CSS120324:101217-182411	CSS1012-18	10:12:17	-18:24:11	2012 May 30	SOAR	3600	D/IP
SSS110504:101240-325831	SSS1012-32	10:12:40	-32:58:31	2012 Apr 21	SOAR	3600	D
CSS110225:112749-054234	CSS1127-05	11:27:49	-05:42:34	2012 Mar 18	SOAR	1440	P
CSS071218:124027-150558	CSS1240-15	12:40:27	-15:05:58	2012 Mar 17	SOAR	3600	E
MLS110329:125118-020208	MLS1251-02	12:51:18	-02:02:08	2012 Apr 23	SOAR	8100	E
SSS110724:135915-391452	SSS1359-39	13:59:15	-39:14:52	2012 Apr 22	SOAR	1440	D/IP
MLS110301:140203-090329	MLS1402-09	14:02:03	-09:03:29	2012 Apr 23	SOAR	8100	E
MLS100617:140447-152226	MLS1404-15	14:04:47	-15:22:26	2012 Mar 17	SOAR	3600	E
SSS100507:144833-401052	SSS1448-40	14:48:33	-40:10:52	2012 Mar 26	OPD	1800	PRG
CSS100216:150354-220711	CSS1503-22	15:03:54	-22:07:11	2012 Mar 16	SOAR	3600	P
MLS110526:151937-130602	MLS1519-13	15:19:37	-13:06:02	2012 Mar 18	SOAR	3600	RRL
MLS110609:160907-104013	MLS1609-10	16:09:07	-10:40:13	2012 Apr 22	SOAR	3600	P
CSS080606:162322+121334	CSS1623+12	16:23:22	+12:13:34	2012 Apr 22	SOAR	8100	D
SSS100804:163911-235804	SSS1639-23	16:39:11	-23:58:04	2012 Sep 03-04	OPD	2700	PRG
CSS110623:173517+154708	CSS1735+15	17:35:17	+15:47:08	2012 Apr 23	SOAR	1440	D
1RXS J174230.1-042953	1RXS1743-04	17:43:20	-04:29:57	2012 Mar 16	SOAR	720	P
1RXS J192926.6+202038	1RXS1929+20	19:29:28	+20:20:35	2012 Apr 23	SOAR	1440	D
SSS110625:194030-633056	SSS1940-63	19:40:30	-63:30:56	2012 Sep 03	OPD	2700	PRG
SSS100805:194428-422029	SSS1944-42	19:44:28	-42:02:09	2012 Apr 22	SOAR	3600	P
SSS110526:195648-603430	SSS1956-60	19:56:48	-60:34:30	2012 Apr 21	SOAR	720	P
USNO-A2.0 0825-18396733	USNO0825-18	20:31:38	-00:05:11	2012 May 20-Jun 25	SOAR	3600	P
SSS110526:204247-604523	SSS2042-60	20:42:47	-60:45:23	2012 Aug 10	SOAR	3600	HA
MLS100706:204358-194257	MLS2043-19	20:43:58	-19:42:57	2012 Aug 10	SOAR	540	D/IP
MLS111021:204455-162230	MLS2044-16	20:44:55	-16:22:30	2012 Sep 03	OPD	2700	RRL
MLS101102:205408-194027	MLS2054-19	20:54:08	-19:40:27	2012 Aug 10	SOAR	1800	D/IP
CTCV J2056-3014	CTCV2056-30	20:56:52	-30:14:38	2012 Sep 04	OPD	2700	D/IP
CSS110513:210846-035031	CSS2108-03	21:08:46	-03:50:31	2012 May 20-Jun 25	SOAR	3600	D
MLS100620:213227-150523	MLS2132-15	21:32:27	-15:05:23	2012 Aug 10	SOAR	900	RRL
CSS100624:220031+033431	CSS2200+03	22:00:31	+03:34:31	2012 Aug 14	SOAR	3600	D/IP
1RXS J222335.6+074515	1RXS2223+07	22:23:34	+07:45:19	2012 Aug 25	SOAR	8100	D
MLS100906:223034-042347	MLS2230-04	22:30:34	-04:23:47	2012 Aug 25	SOAR	1440	E
SSS110720:224200-662512	SSS2242-66	22:42:00	-66:25:12	2012 Sep 03-04	OPD	2700	D/IP
CSS111021:231909+331540	CSS2319+33	23:19:09	+33:15:40	2012 Sep 04	OPD	2700	D/IP

^aP: polar candidate, D: disk system, D/IP: IP candidate, HA: system with high-state accretion disk, N: Nova, RRL: RR Lyrae star, PRG: Mira or low-amplitude Pulsating Red Giants star, E: extragalactic source.

3. TEMPORAL ANALYSIS OF CRTS DATA

We performed time series analyses of the CRTS photometric data for all objects except the extragalactic (Sec. 4.7), to search for periodic signals. The sampling of the CRTS light curves has a typical minimum separation between measurements of $\Delta t = 0.01$ days. This means that if the time series was equally spaced with this sampling, the Nyquist frequency would be $F_{Ny} = 1/2\Delta t = 50$ d⁻¹. The total span of the observations is ≈ 3000 d, which implies (again for equally spaced sampling) a frequency step $\Delta F = 1/T = 3.3 \times 10^{-4}$ d⁻¹. The number of frequencies to be examined for coherent signals is $N = F_{Ny}/\Delta F \approx 1.5 \times 10^5$. We choose to examine a grid of $N = 10^6$ frequencies giving some flexibility to possible effects coming from the nonuniform sampling of the time series.

We used the Discrete Fourier Transform (DFT, Deeming 1975; Lomb 1976), the Lomb-Scargle (LS, Lomb 1976; Scargle 1982) including its Bayesian formalism implementation (Mortier et al. 2015), the String-Length (SL, Dworetsky 1983; Clarke 2002) and the Phase Dispersion Minimization (PDM, Stellingwerf 1978) methods for signal search, depending on each data sample. These tools can be classified in two groups, those of the DFT family (DFT, LS) based on Fourier transform and those based on phase diagram methods (SL, PDM), which have the advantage of being sensitive even for highly non-sinusoidal signals, as in the case of eclipsing binaries or pulsating stars. Our implementation of the String-Length method has an improvement: instead of measuring only the Δy distances in the phase diagram, we measure a variable proportional to $\sqrt{\Delta y^2 + \Delta \phi^2}$. With this approach, the method behaves well even when there are large gaps of data in the phase diagram. The relevant results are presented in each respective object section.

4. OBJECT CLASSIFICATION

Exploratory spectra of 47 targets (see Figure 1) were obtained in order to identify characteristic features of magnetic CVs. Most of the objects are CVs, many are magnetic CVs, but we also found RR Lyrae, pulsating red giants, and extragalactic objects. We have searched for counterparts in

other wavelengths and verified if the objects are included in specific catalogs. The relevant counterpart information is presented in the following discussion for each object, which are grouped following the proposed classification.

4.1. Polar Candidates

This section comprises the polar candidates, or diskless accretors. Their optical light curves do not show outbursts originated in the accretion disk, while their spectra present signs of high ionization mass accretion. These include a steep blue continuum, the presence of He I, He II 4686 Å and the C III/N III blend in emission and H β more intense than H α . The other mCVs - IP candidates - are placed in the next section together with other disk-accretion systems. Table 2 presents the FWHM and the equivalent width of the Balmer and He II 4686 Å lines of the objects classified as CVs in this article. These numbers are useful for the classification of magnetic CVs: they are characterized by H β equivalent width larger than 20 Å and He II 4686 Å/H β larger than 0.4, according to Silber (1992) as cited by Mukai's Intermediate Polars Homepage³.

4.1.1. *MLS0227+13 (MLS110213:022733+130617)*

The CRTS light curve ranges from 16.5 to 19.5 in timescales of days. The spectrum is typical of polars with H β more intense than H α . The He II 4686 Å emission line is as intense as H β (Table 2) and the high-ionization Bowen C III/N III is also present. In a follow-up observational study, Silva et al. (2015) confirmed MLS0227+13 as an eclipsing polar with an orbital period of 3.787 h, using polarimetric, photometric and spectroscopic data. The system has no X-ray counterpart, which can be explained by a large distance (Silva et al. 2015).

4.1.2. *CSS0357+10 (CSS091109:035759+102943)*

CSS0357+10 was detected as a transient by CRTS on 2009 November 9. The V magnitudes are highly variable, spanning from 16.5 to 21 in short timescales. Schwope & Thinius (2012) performed a time-resolved photometric study of this target and found a periodicity of 114 min with 0.8

³<http://asd.gsfc.nasa.gov/Koji.Mukai/iphome/iphome.html>

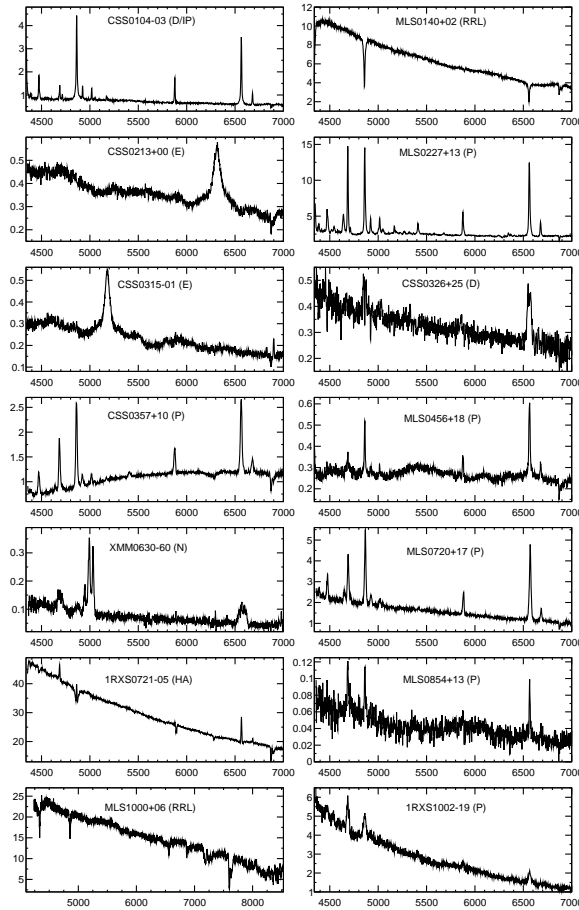


Fig. 1.— Exploratory spectra arranged by right ascension. The vertical axes are F_λ in units of 10^{-16} erg $\text{cm}^{-2} \text{s}^{-1} \text{\AA}^{-1}$ and the horizontal axes are Wavelength, in \AA .

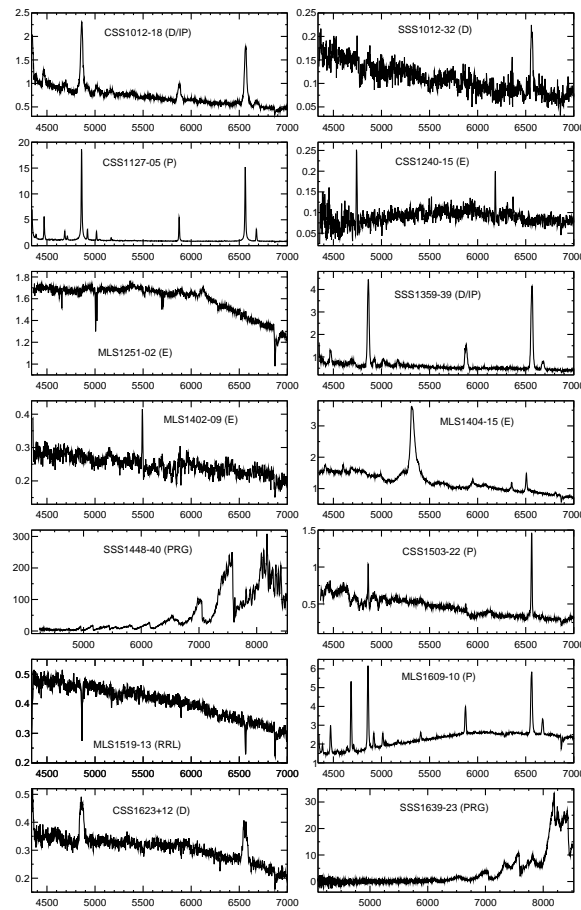


Fig. 1.—Continued

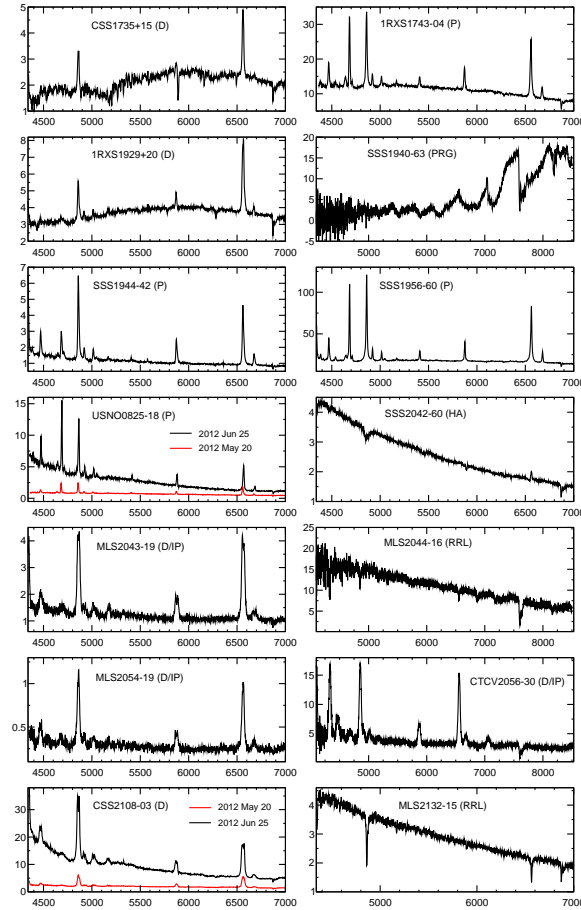


Fig. 1.—Continued

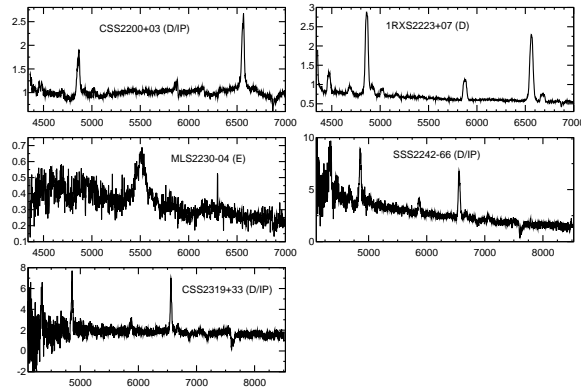


Fig. 1.—Continued

mag amplitude, interpreted as the orbital period of a non-eclipsing polar candidate. This object is also detected in X-rays (ROSAT, XMM-Newton), presenting large variability (Schwope & Thinius 2012).

The exploratory spectrum is dominated by intense Balmer and He II 4686 Å lines and also presents He I and weak He II 5411 Å, Bowen C III/N III complex and Fe II 5170 Å emissions. The Balmer and He II 4686 Å lines are asymmetric, with extended red wings, and H β is more intense than H α (Table 2), confirming the polar classification.

4.1.3. *MLS0456+18 (MLS101203:045625+182634)*

This object was detected as a variable star on 2013 December 10 by the CRTS. Its light curve spans from 18.5 to 21.5 mag, reaching 1 mag variation amplitude in timescales of hours. Narrow Balmer emission lines dominate the exploratory spectrum, which also presents He I and He II 4686 Å lines. This last line is composed of a broad component (EW= -18) superposed on a very narrow central emission (EW= -1). This multi-component line profile, the EW of H β , and the ratio between He II 4686 Å and H β (Table 2) suggest a mCV classification. The continuum shows humps that may be associated to cyclotron harmonics. This property and the absence of an X-ray counterpart are consistent with a low accretion-rate polar or a pre-polar system (e.g., Schmidt et al. 2005). Our search for periodicities in the CRTS data yielded a period of 0.09851 d and the corresponding phase diagram (Figure 2) is compatible with a polar light curve. The period (=2.36 h) places MLS0456+18 inside the period gap of CVs. As many objects of this work, a more specific classification demands more observations.

4.1.4. *MLS0720+17 (MLS101226:072033+172437)*

The CRTS light curve of MLS0720+17 presents 0.5 mag amplitude variability around 18.5 mag, occasionally dropping to 20-21 mag, possible during eclipse events (Drake et al. 2014). The Goodman exploratory spectrum is typical of polars, with Balmer, He II 4686 Å, C III/N III and He I narrow emission lines superposed on a continuum with a blue slope. The He I line profiles are asymmetric with extended blue wings in this spectrum.

No X-ray source was found near its coordinates. The time series analysis applied to the CRTS data does not show any period that could explain the low flux incursions.

4.1.5. *MLS0854+13 (MLS120127:085402+133633)*

This target matches a blue stellar counterpart in SDSS, with $u = 20.18$, $g = 20.58$, $r = 20.43$, $i = 20.28$, and $z = 20.06$ in DR8. It presents two brightness levels with average 19.7 and 21.5 mag in CRTS data. It is associated with the X-ray source 1WGA J0854.0+1336 in the WGA Catalog of ROSAT Point Sources⁴. This object is also classified as BOSS J085402.10+133632.8, a $z=2$ QSO in the MILLIQUAS Catalog V4.7⁵. However, our spectrum is completely consistent with a Galactic object. Our average spectrum is similar to the spectrum of a polar in low accretion state, with cyclotron humps and emission lines of He II 4686 Å, H β and H α over a blue slope. No periodicity was found in the CRTS time series analysis.

4.1.6. *1RXS1002-19 (1RXS J100211.4-192534)*

This source was discovered by ROSAT (Beuermann & Thomas 1993) and classified as a polar with an X-ray orbital period of 106 min (Beuermann & Schwope 1994). 1RXS1002-19 was observed with XMM-Newton (Ramsay & Cropper 2003) and the resulting X-ray light curve suggests that the source of radiation is located in one hemisphere of the WD. Modeling of the X-ray spectrum yields a WD mass close to $0.5 M_{\odot}$.

Our optical spectrum of 1RXS1002-19, the first of this source, has a strong blue slope and the He II 4686 Å line is more intense than H β , which in turn is more intense than H α (Table 2). He I features are also present in emission. The widths of the H β and He II 4686 Å lines are around 2000 km s $^{-1}$ (Table 2), which is unusual for a polar. The equivalent width of H β is 11 Å, smaller than the Silber (1992)'s criterion for a magnetic classification (20 Å). Our spectrum converts to V = 18 mag. This locates the object in the polar systems region of X-ray counts rates versus optical mag diagram, according to Figure 2 of Beuermann & Thomas (1993).

⁴<http://heasarc.gsfc.nasa.gov/wgacat/>

⁵<http://heasarc.gsfc.nasa.gov/w3browse/all/milliquas.html>

4.1.7. *CSS1127-05 (CSS110225:112749-054234 = SSS120624:112749-054236)*

CSS1127-05 has a blue point source counterpart in SDSS, with $u = 20.00$, $g = 20.12$, $r = 20.09$, $i = 20.28$ and $z = 20.15$ in DR8. The CRTS light curve clearly shows two distinct brightness states with average magnitudes of 18.5 and 20.5. The exploratory spectrum has high signal to noise ratio, displaying strong and narrow Balmer lines in emission on a flat continuum, besides less intense He II 4686 Å and He I. H β is more intense than H α . The H α EW (204 Å) is the largest among the objects we classify as CV (Table 2). In spite of the low ratio between He II 4686 Å and H β (0.16), considering the Silber (1992)'s criterion, we suggest it is a polar due to the presence of high and low-brightness states. No significant period was found in the CRTS data. The system has no X-ray counterpart.

4.1.8. *CSS1503-22 (CSS100216:150354-220711 = SSS100512:150354-220710)*

The light curve of CSS1503-22 presents two alternating brightness states at average magnitudes 19.5 and 17.5, both states with dispersion of 1 to 1.5 mag. Woudt et al. (2012) performed photometric monitoring of CSS1503-22 in March and April 2010 on five runs summing up to 15 h of observations when it was at high state. They found a period of 133.38 min and, for its photometric behavior and the detection as a Swift X-ray source, they suggested it to be a polar. The flux of our SOAR spectrum corresponds to 19.7 mag, which is consistent with the CRTS low state. The spectrum displays narrow Balmer lines, possibly with blue wings, and H β being half the intensity of H α (Table 2). The He I 5876 Å is also present. The spectrum presents quite peculiar absorption features from 4500 to 6000 Å, some of which occurring at typical wavelengths of TiO bands from a M2 – M5 secondary star (see, for instance, Mennickent et al. 2002 and Gray & Corbally 2009). The absorptions near H β have positions, profiles and depths which are more challenging to understand, and hamper the detection of possible He II 4686 Å or Bowen complex emission. The EW of H β is 16 Å, slightly smaller than 20 Å of the Silber (1992)'s criterion, but the cited absorptions can affect the accuracy of the

measured EW.

4.1.9. *MLS1609-10 (MLS110609:160907-104013)*

The CRTS light curve of this object has measurements scattered from 16.8 to 20.5 mag. The exploratory spectrum presents intense and narrow Balmer lines in emission. These lines are slightly asymmetrical, presenting extended red wings. H β is more intense than H α , while He II 4686 Å is almost as intense as H β (Table 2). The Bowen complex at 4630-4650 Å is clearly visible. The spectrum shown in Figure 1 is the average of three consecutive spectra, obtained with 20 min intervals. They show a remarkable variability in the continuum, hence they are individually presented in Figure 3. We performed a 3.6 h span photometric time-series of this source on 2014 April 28, using the 1.6 m P&E telescope at OPD and the Andor iKon-L936BV camera, obtaining 39 images with 240 s exposure time through V filter. The differential photometry was converted to V magnitude using as reference the star NOMAD1 0793-0295201, with $m_v = 16.51$ (Zacharias et al. 2004).

The OPD lightcurve is consistent with a polar classification and shows a modulation with a period around 0.077 d and 0.60 ± 0.05 mag amplitude. In the search for periodic signals in the CRTS data, the PDM method yielded a period of $P = 0.075439 \pm 0.000001$ d, compatible with the OPD period. Figure 4 shows both OPD and CRTS light curves folded with $P = 0.075439$ d and epoch $T_0 = 2\,456\,776.7108$ HJD. The average magnitude of the OPD data is V=21.3, therefore the source was caught in a very low state, whereas the individual spectra correspond to 17.8 and 19 V mag. The system has no X-ray counterpart.

4.1.10. *1RXS1743-04 (1RXS J174320.1-042953 = USNO-B1.0 0855-0326594)*

This CV was discovered by Denisenko & Sokolovsky (2011) among X-ray sources in the ROSAT catalog. Denisenko & Martinelli (2012) performed time-resolved photometry and suggested the target to be a polar or IP, based on the amplitude (0.8 mag in white light) and shape of the light curve. They determined an orbital period of 2.08 h.

Our exploratory spectrum is typical of polars, with very intense He II 4686 Å and H β more in-

tense than $\text{H}\alpha$. The C III/N III complex is also present and the continuum increases to the blue. Our spectrum corresponds to $V = 16.3$ mag.

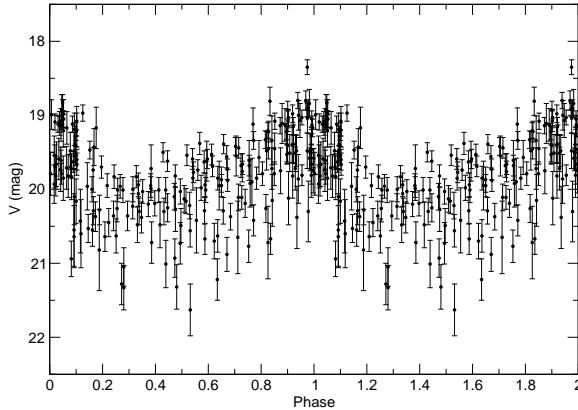


Fig. 2.— CRTS light curve of MLS0456+18 folded with the period of 0.09851 d.

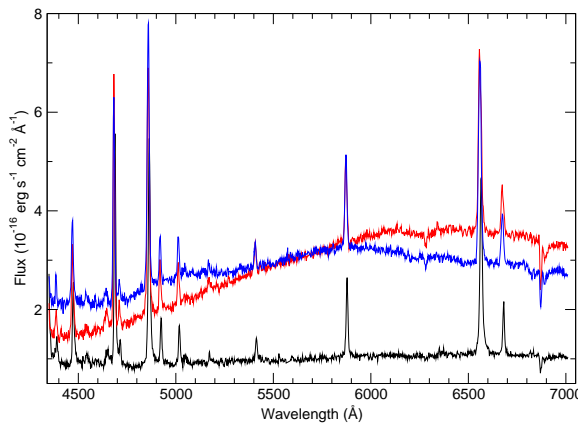


Fig. 3.— Three consecutive (black, red, blue) spectra of MLS1690-10 obtained with 20 min intervals.

4.1.11. *SSS1944-42 (SSS100805:194428-420209)*

The CRTS light curve of this object presents two brightness levels separated by 2 mag and short timescale variability. Coppejans et al. (2014) performed photometric monitoring during the bright state and classified it as a polar for its light curve, which is modulated with a period of 1.53 h. Our spectrum was obtained in the low-brightness state ($V \approx 19$ mag) and presents narrow, single peaked Balmer, He I and He II 4686 Å emission features over a blue continuum. The Balmer and He II lines have extended red wings and $H\beta$ is 35% more intense than $H\alpha$ (Table 2). The C III/N III Bowen complex at 4640 Å and the lines of Fe II 5169 Å and He II 5412 Å are also visible. The system has no X-ray counterpart.

4.1.12. *SSS1956-60 (SSS110526:195648-603430)*

This source presents many kinds of variability in the CRTS light curve: long (years) and short (one month) term variations between magnitudes 18 and 15, and 1 mag variations in timescales of few days. SSS1956-60 is classified as the nova-like CV V348 Pav (Downes et al. 2001) and is also identified as V1956-6034, a polar candidate by its spectrum (Drissen et al. 1994). Our exploratory spectrum displays narrow Balmer, He I and He II emission lines. The line of He II 4686 Å is almost as intense as $H\beta$, which in turn is more intense than $H\alpha$ (Table 2). Also present in the spectrum are the lines of the Bowen complex, He II 4541 and 5412 Å and Fe II 5169 Å. In the spectrum obtained in 1992 by Drissen et al. (1994), the ratio of the intensities $H\beta/\text{He II } 4686 \text{ \AA}$ is 0.25, much lower than the value of 0.91 we measured in our spectrum from 2012. An X-ray counterpart was detected with 1.8 counts sec^{-1} total band count rate at these coordinates by XMM-Newton in the slew data mode, and was registered as XMMSL1 J195647.7-603425 in the XMM-Newton Slew Survey Clean Source Catalog (Saxton et al. 2008).

4.1.13. *USNO0825-18 (USNO-A2.0 0825-18396733)*

The discovery of this polar candidate is reported by Kryachko et al. (2010). From R light curve, they obtained an orbital period of 0.0848 d (2.035 h), while their spectrum shows He II 4686 Å almost as intense as $H\beta$ and also He I and the Bowen blend. Afanasiev et al. (2015) performed

polarimetric observations of this source and found variable circular polarization reaching -31% .

We obtained exploratory spectra of USNO0825-18 in two occasions in 2012, 35 days apart. In the second run, the flux in the blue was 6 times more intense than in the first observation (Figure 1) and the He II 4686 Å to $H\beta$ intensity ratio increased from 0.97 to 1.23 (Table 2).

4.2. Systems with Disks

The objects presented here show indication of accretion driven by disks, like broad emission lines, double-peaked Balmer emission profiles and evidences of DN type eruptions in the light curves. Intermediate polar candidates, being disk systems, are also in this group and their optical spectra may sometimes be virtually indistinguishable from the spectrum of a DN in quiescence, especially for the short-period IPs. CVs may be detected as X-ray sources, having the mCVs the highest X-ray to optical flux ratios followed by dwarf novae in quiescence (e.g., Beuermann & Thomas 1993; Fertig et al. 2011; Szkody et al. 2011).

4.2.1. *CSS0104-03 (CSS091009:010412-031341)*

This object was discovered and classified as an eclipsing CV by CRTS on 2009 October 9 in a single outburst when it reached $V=17.2$ mag. CRTS data span from 2005 to 2015, during which the object showed average $V=19$ mag and ~ 1 mag amplitude in timescales of hours, with occasional 21 mag incursions. Another outburst was recorded by the All Sky Automated Survey (ASAS; Pojmanski 2002) at 16.39 mag on 2013 August 27 (Ohshima 2013). Szkody et al. (2014) present a spectrum with strong emission Balmer lines obtained on 2013 September 3 and classify the object as a dwarf nova, possibly eclipsing due to the dispersion of CRTS quiescent light curve. This spectrum was taken in a state brighter than the quiescent flux in the CRTS light curve. The SDSS DR9 counterpart of CSS0104-03 presents $u = 19.2, g = 19.5, r = 19.1, i = 18.8$ and $z = 18.9$.

Our Goodman spectrum shows narrow and single peaked Balmer, He I and He II 4686 Å emission lines, $H\beta$ being 1.26 times more intense than $H\alpha$ (see Table 2). The continuum is flat with a slight slope to the blue. The Balmer lines have extended wings and are slightly asymmetrical. The average

TABLE 2

FULL WIDTH AT HALF MAXIMUM (FWHM^a) AND EQUIVALENT WIDTH (EW) OF He II 4686 Å, H β AND H α EMISSION LINES OF THE OBJECTS CLASSIFIED AS POLARS AND DISK SYSTEMS.

Object	FWHM He II (km s ⁻¹)	-EW He II (Å)	FWHM H β (km s ⁻¹)	-EW H β (Å)	FWHM H α (km s ⁻¹)	-EW H α (Å)	He II/H β
CSS0104-03	490	6	580	59	450	63	0.32
MLS0227+13	630	47	700	66	600	76	1.01
CSS0326+25	2380	47	...
CSS0357+10	1040	22	1050	40	900	30	0.73
MLS0456+18	750	13	730	20	690	23	0.71
MLS0720+17	1040	19	940	32	850	65	0.79
1RXS0721-05	530	1	420	1	400	4	0.83
MLS0854+13	930	15	810	24	490	30	1.06
1RXS1002-19	1850	12	2090	11	1200	10	1.17
CSS1012-18	p ^b	p	1710	64	1250	78	...
SSS1012-32	2500:	21	1120	53	...
CSS1127-05	540	14	550	183	450	204	0.16
SSS1359-39	p	p	1240	157	1030	197	...
CSS1503-22	490	16	490	44	...
MLS1609-10	730	29	870	40	840	26	0.87
CSS1623+12	2670	19	2370	28	...
CSS1735+15	1250	23	840	24	...
1RXS1743-04	760	21	880	32	730	36	0.96
1RXS1929+20	p	p	1000	14	1020	30	...
SSS1944-42	950	16	890	65	770	65	0.46
SSS1956-60	600	48	700	80	570	59	0.91
USNO0825-18 (May 20)	630	22	660	22	630	42	0.97
USNO0825-18 (Jun 25)	580	27	690	26	640	38	1.23
SSS2042-60	860	1	630	2	...
MLS2043-19	p	p	2070	87	1650	91	...
MLS2054-19	p	p	1700	84	1311	93	...
CTCV2056-30	p	p	2430	124	1850	160	...
CSS2108-03 (May 20)	p	p	1720	51	1520	81	...
CSS2108-03 (Jun 25)	p	p	1930	66	1690	92	...
CSS2200+03	p	p	2010	32	1320	43	...
1RXS2223+07	p	p	2010	90	1720	128	...
SSS2242-66 (Sep 03)	p	p	2200	71	1890	125	...
SSS2242-66 (Sep 04)	p	p	2300	56	1610	62	...
CSS2319+33	p:	p:	1360	144	1130	85	...

^aThe FWHM were measured from Voigt profile fitting.

^bThe symbol p means that the line is present in the spectrum but its S/N is low and no measurements were possible.

continuum flux in our spectrum is a factor of 4 less intense than the continuum flux in the spectrum published by Szkody et al. (2014), in which the line of He II 4686 Å is only marginally detected. CSS0104-03 has the highest He II 4686 Å EW among our sample of disk-accretion systems. Our spectrum has a flux level around 19 mag in the V band, hence it is consistent with the mean level of the CRTS light curve.

Our time series analysis of the CRTS data does not reveal any period which could explain the low flux incursions as eclipses. The small widths of the lines are also inconsistent with an eclipsing system. So the system could be a near face-on dwarf nova. However, this classification does not explain the low flux measurements, the two-component emission lines, and the He II 4686 Å line behavior, since its intensity was expected to be higher at the spectrum from Szkody et al. (2014) taken at a brighter state. The object has no X-ray counterpart. If we suppose that its low brightness is due to its distance, it is possible that its X-ray luminosity is not high enough to allow the object detection in X-ray surveys. This seems to be true for MLS0227+13 (Silva et al. 2015). Therefore, a magnetic classification is a good compromise taking into account the observations. Moreover, if the brightest points correspond to eruptions, it could be an IP system, possibly similar to GK Per or EX Hya. Spectroscopic time series would be useful to a definite classification of this system.

4.2.2. *CSS0326+25 (CSS090922:032603+252534)*

The light curve of this source, obtained by CRTS, has a large amplitude of variation, from 18.5 to 20 mag. It might be originated by flips between two brightness states. The average spectrum presents broad emission lines of H α and H β . H α shows a profile with two peaks, while H β is quite peculiar, with a strong central absorption at the rest position of the line in the middle of the broad emission. He I lines are visible in absorption at 4471 and 4922 Å, despite the low S/N ratio at the continuum, and other lines of He I are not seen. Also marginally detectable are absorption lines of Na I 5890 Å and the diffuse interstellar band (DIB) at 6284 Å. Our time series analysis does not reveal any remarkable result.

4.2.3. *CSS1012-18 (CSS120324:101217-182411 = SSS110203:101217-182411)*

This CRTS source has been discovered by SSS on 2011 February 3, receiving the ID SSS110203:101217-182411 and was later detected by CSS, on 2012 March 24, when it was assigned as CSS120324:101217-182411. The CRTS light curves varies between 18-20 mag with sporadic outbursts reaching 16-17 mag. Our spectrum displays a blue slope and broad He I and Balmer emission lines, H β being more intense than H α . He II 4686 Å is present as well. The spectrum flux corresponds to approximately 19.3 mag in V band, consistent with the quiescent flux level. Coppejans et al. (2016) classify it as a dwarf nova with 3 detected outbursts. Its spectrum resembles the spectrum of the IP candidate CTCV2056-30 (see section 4.2.11) and short-period IPs like SDSS J2333 (Southworth et al. 2007; Szkody et al. 2005) and HT Cam (Kemp et al. 2002), so we suggest that it is a member of this class. The String-Length spectrum of the CRTS data shows some structure, but it does not translate into discernible features in the folded diagrams.

4.2.4. *SSS1012-32 (SSS110504:101240-325831)*

This object is associated to the X-ray source 1RXS J101239.6-325839. The CRTS light curve has short term (days) variability between 17.3 and 19.5 mag, but no periodicity was found. Moreover, the CRTS light curve does not present DN-type eruptions. The spectrum has low S/N. The line of H α is clearly seen as a broad emission line while H β is weak. The continuum is quite blue. Despite not showing spectral features characteristic of magnetic systems, its ROSAT colors match those sources. The spectrum shows modulations that might be due to absorptions features of a red secondary, but we could not associate their wavelengths to features usually found in M stars.

4.2.5. *SSS1359-39 (SSS110724:135915-391452)*

SSS1359-39 was discovered by CRTS and its light curve has a quiescent brightness level at 19 mag with a dispersion of 1 mag, and sporadic outbursts at magnitudes 14 - 15. The period search had negative results. This source is correlated to the X-ray source 1RXS J135915.6-391447. The exploratory spectrum show features related to an ac-

cretion disk, with intense and broad Balmer emission lines ($\text{FWHM} > 1000 \text{ km s}^{-1}$ - Table 2) along with He I, Fe I, Fe II and He II 4686 Å, and is very similar to the spectrum of the IP candidate CTCV2056-30 (section 4.2.11).

4.2.6. *CSS1623+12 (CSS080606:162322+121334)*

Photometric monitoring from CRTS yields a flat light curve at mag 17 with rapid and short occasional decreases of 3 magnitudes. SDSS registers this object as a blue point source with $u = 21.85, g = 21.88, r = 21.42, i = 21.38$ and $z = 21.25$. Drake et al. (2014) obtained a spectrum of this object in high-accretion state, with broad Balmer absorptions on a blue continuum. Our SOAR spectrum was obtained in a faint state ($V \approx 20.2$ mag) and shows the Balmer lines in emission. These lines are broad and with double peak profiles, indicating a possible high orbital inclination. Therefore the system may be eclipsing, which would explain the rapid and deep drops in the CRTS light curve. The time series analysis of the CRTS data does not reveal any clear periodicity, probably because most of the fainter points are limits and are not included in the photometric CRTS data. If the object is indeed eclipsing, our spectrum (exposure time of 2700 s) should be taken predominantly during the eclipse, which should be therefore relatively long. This source could be alternatively interpreted as a VY Scl novalike for its spectral and photometric behavior.

4.2.7. *CSS1735+15 (CSS110623:173517+154708)*

The light curve obtained by CRTS is nearly flat around 17 and 17.5 mag with one episodic measurement at 14.3 mag and another at 18 mag. Thorstensen & Skinner (2012) obtained one spectrum in September 2011 in which H α is visible in emission together with a K-star feature at 5168 Å. Kato et al. (2013) found two photometric periods (0.05436 d and 0.05827 d) but the exact interpretation of these is still not clear, but one could be related to a superhump. Spectral observations by Drake et al. (2014) reveal CSS1735+15 in eruption with a steep blue continuum and absorption features of H γ and H δ . The SOAR spectrum has the same flux level as the spectrum from Thorstensen & Skinner (2012) and displays typical features of a K star and Na I absorption together with emission lines of H I and He I. Our

spectrum has not enough coverage to propose a luminosity class, but it is not inconsistent with an evolved object.

4.2.8. *1RXS1929+20 (1RXS J192926.6+202038 = USNO-B1.0 1103-0421031)*

This is another CV discovered by Denisenko & Sokolovsky (2011) among X-ray sources in the ROSAT catalog and which was classified as a possible dwarf nova by its X-ray hardness ratio. Our exploratory spectrum is reddened, with emission lines of H I, He I and indication of He II 4686 Å or C III/N III, besides two DIBs at 5780 and 6284 Å. The feature at 5577 Å is associated to bad subtraction of the telluric [O I] line.

4.2.9. *MLS2043-19 (MLS100706:204358-194257)*

MLS2043-19 was discovered as a transient optical source by CRTS. Its light curve has a quiescent level at ~ 19.5 mag and four registered outbursts, reaching 15 mag. The CRTS data do not present any evidence of eclipse or periodicity. The SOAR spectrum, on the other hand, presents broad and double-peaked Balmer and He I emission lines, which suggest a high orbital inclination system, besides weak He II 4686 Å or C III/N III emission features over a blue continuum. It also reminds the spectrum of the IP candidate CTCV2056-30 presented in section 4.2.11.

4.2.10. *MLS2054-19 (MLS101102:205408-194027 = CSS090829:205408-194027)*

This object, discovered by CRTS, has a bimodal light curve with a low-brightness state at 19.5 mag with 1 mag variation and several outbursts reaching between 18 and 16 mag. Coppejans et al. (2014) found a photometric period of 0.09598 d, suggesting it to be associated to superhumps visible in the light curves, and estimated an orbital period of 0.0917 d. Our exploratory spectrum shows double-peaked H β emission more intense than H α , besides He I and He II 4686 Å (and possibly He II 4542 Å), being similar to the spectrum of the IP candidate CTCV2056-30, which suggests possible magnetic accretion.

4.2.11. *CTCV2056-30 (CTCV J2056-3014 = 1RXS J205652.1-301433)*

This object was discovered by Augusteijn et al. (2010) during the Calán-Tololo Survey. Their low-resolution spectra present Balmer and He I emission lines over a blue continuum. The radial velocity curves provided a period of 1.76 h assumed as the orbital modulation, while photometric monitoring yields an additional modulation with $P=15.4$ min, leading to a probable IP classification. Those authors also report some likely dwarf nova outbursts registered by the ASAS and the ROSAT X-ray detection as 1RXS J205652.1-301433. Our spectrum shows $H\beta$ as intense as $H\alpha$ and relatively intense He I and weak He II 4686 Å lines. The continuum is flatter and around 3 times less intense in the blue than the spectrum from Augusteijn et al. (2010). This spectrum is quite similar to the spectra of short-period IPs like SDSS J2333 (Southworth et al. 2007; Szkody et al. 2005), HT Cam (Kemp et al. 2002) and DW Cnc (Patterson et al. 2004; Rodríguez-Gil et al. 2004), among others. These objects present spectra that are indistinguishable from quiescent dwarf nova spectra and, therefore, show that a single optical spectrum is not enough to confirm the IP nature of a source. The definite IP classification demands the detection of the white dwarf spin period not synchronized to the orbital modulation.

4.2.12. *CSS2108-03 (CSS110513:210846-035031)*

This system was discovered by CRTS in May 2011, displaying a light curve with a quiescent level at 18 mag and outbursts reaching 15 mag. Coppejans et al. (2014) performed time-resolved photometry in October 2011 and found eclipsing light curves, deriving an orbital period of 0.15699 d. A compatible period of 0.1569268 d was determined independently by Drake et al. (2014) from the photometric data from CRTS itself, in both quiescence and outburst.

We obtained two exploratory spectra of CSS2108-03, in 2012 May 20 and 2012 June 25, and found characteristic features of a disk system. Emission lines of H I and He I are broad and have pronounced double peak profiles, supporting the high orbital inclination shown by the eclipses. The flux in June was a factor of five higher than in May, and the continuum was steeper to the blue.

4.2.13. *CSS2200+03 (CSS100624:220031+033431)*

This object was discovered by CRTS and suggested to be a polar type CV in the CRTS circulars⁶. Its light curve presents a quiescent level with long term (years) variability ranging from 18 to 19.5 mag and several outbursts reaching about 16.5 mag. de Budè (2011) performed photometric follow-up observations, which yield non-eclipsing light curves (within a maximum time span of 3.6 h) dominated by flickering with less than 0.5 mag amplitude.

Our exploratory spectrum displays broad Balmer and He I emission lines with double peak profiles, which are more conspicuous in the He I lines. The presence of a disk evidenced by the double peak lines discards the polar classification. He II 4686 Å and C III/N III are weak but present. The continuum shows absorption features which could be associated to a cool secondary. The spectral features are somewhat similar to the spectrum of CTCV2056-30.

4.2.14. *1RXS2223+07 (1RXS J222335.6+074515 = USNO-B1.0 0977-0743560)*

Also selected as a new CV from the ROSAT catalog, 1RXS2223+07 presents a DN light curve with outbursts 2 mag above the average 19.5 mag quiescent level (Denisenko & Sokolovsky 2011). Our spectrum presents broad Balmer and He I emission lines, besides He II 4686 Å, on a slightly red continuum.

4.2.15. *SSS2242-66 (SSS110720:224200-662512 = 1RXS J224150.4-662508)*

This source presents a CRTS light curve varying between 16.5 and 18 mag with two outbursts reaching 15-15.5 mag. It matches the X-ray source 1RXS J224150.4-662508. Our spectrum, obtained at OPD, shows emission lines of $H\alpha$, $H\beta$, He I and He II 4686 Å over a slightly blue continuum. Its spectrum is very similar to the spectrum of the IP candidate CTCV2056-30 described above which, as in this case, also presents outbursts and X-ray detection. These similarities may indicate an IP nature for SSS2242-66.

⁶<http://nesssi.cacr.caltech.edu/catalina/Circulars/1006241041184114393.html>

4.2.16. *CSS2319+33 (CSS111021:231909+331540)*

CSS2319+33 has a highly variable CRTS light curve with short and long timescales, ranging from 16.5 to 19.5 mag, but it does not show any outburst. It matches a blue source at SDSS DR8, with $u = 17.45, g = 17.79, r = 17.68, i = 17.36$ and $z = 17.02$ and also matches the ROSAT source 1RXS J231909.9+331544. Despite being noisier, the OPD spectrum is very similar to the spectrum of SSS2242-66, which in turn resembles the spectrum of CTCV2056-30, so we consider it as an IP candidate.

4.3. Systems with Disks in High Accretion State

4.3.1. *1RXS0721-05 (1RXS J072103.3-055854 = USNO-B1.0 0840-0137592)*

Denisenko & Sokolovsky (2011) identified this system as USNO-B1.0 0840-0137592, the optically variable counterpart of an X-ray source in the ROSAT catalog, and suggested a classification as a dwarf nova. Their analysis of archive photographic plates shows that most of the time the system is fainter than 17 mag in B band, but occasionally gets brighter, reaching 16.5 mag. Our exploratory spectrum has a flux in the V band of around 15.3 mag, brighter than in any previous detection, corroborating a dwarf-nova classification. Our spectrum is typical of a dwarf nova (DN) in eruption, showing narrow Balmer and He II 4686 Å emission lines superposed on a very blue continuum. During DN eruptions, broad absorption troughs may develop at the base of very narrow Balmer emission cores, mainly in the higher member of the Balmer series - see Warner (1995) and the case of SS Cyg by Hessman et al. (1984). These features are well observed in 1RXS0721-05. Emission lines of He I, the interstellar absorptions lines of Na I 5890 and 5896 Å, and the diffuse interstellar band (DIB) at 6284 Å are also present in our spectrum. If we consider its ROSAT counts rate (Boller et al. 2016) and the quiescent optical magnitude, the object is located in the dwarf-novae region of Beuermann & Thomas (1993)'s Figure 2. Its ROSAT hardness ratios (HR1= 1.000 ± 0.360 and HR2= -0.108 ± 0.276) are also consistent with a dwarf nova (e.g., Hümmerich et al. 2014).

4.3.2. *SSS2042-60 (SSS110526:204247-604523)*

SSS2042-60 has a CRTS light curve with two distinct brightness levels at 18 and 19.5 mag, being observed most of the time at the higher state. No eruption was recorded. Our SOAR spectrum displays a very steep blue continuum with H α in emission and H β in broad absorption with a weak central emission feature. He II 4686 Å is marginally detected and Na I absorption is visible. Our spectrum has a flux equivalent to V = 18 mag, near the brightest state. We suggest the object is a novalike, possibly of VY Scl type due to the fadings in its light curve.

4.4. Nova

4.4.1. *XMM0630-60 (XMMSL1 J063045.9-603110)*

This source was discovered by XMM-Newton in 2011 as a soft X-ray transient (2011 Dec 01) and was suggested to be a Nova for its X-ray softness (Read et al. 2011a). Observations with GROND identified the optical counterpart with $g' = 18.4$ mag and $r' = 19.5$ mag, too faint for a recent Galactic Nova (Kann et al. 2011). The optical source has a blue SED, also atypical for a Nova, with a hint of strong He II emission. Swift observations show a very soft X-ray spectrum with $kT = 48$ eV, 12 times fainter than the XMM-Newton flux obtained 19 days before (Read et al. 2011b). XMM0630-60 was also selected as a blazar candidate, but this classification was not confirmed (Cowperthwaite et al. 2013).

Our spectrum is compatible with a Nova in the nebular phase and displays strong blended lines of [O] III 4959 and 5007 Å. Besides, broad and near rest position emission lines of He II 4686 Å, H β and H α are also present, with multiple narrow components. Our spectrum corresponds to V ≈ 21.8 mag.

4.5. RR Lyrae Stars

RR Lyrae are pulsating stars of spectral class A or F, which vary periodically. They have mass similar to the Sun, but are evolved objects, located in the horizontal branch. RR Lyrae are common variable stars with thousands of known objects, yet they are important standard candles - via period-luminosity relation - to determine distances in our Galaxy and even in the Local Group,

besides being proper objects to stellar evolution studies.

4.5.1. $MLS0140+02$ ($MLS110207:014023+020639$ $= CSS_J014022.8+020639$)

This source was selected from CRTS for its photometric variability. It was classified later on as a RR Lyrae star (Drake et al. 2013) with $P=0.5726$ d. The exploratory spectrum corresponds to A or F spectral type.

4.5.2. $MLS1000+06$ ($MLS110210:100054+065557$ $= CSS_J100053.9+065557 = NSVS\ 13049946$)

This source has a highly variable light curve with measurements spanning from 13.6 to 15 magnitudes. It matches a blue point source in SDSS DR9 and was classified as a RR Lyrae variable by Drake et al. (2013). The spectrum shows narrow Balmer absorptions on a steep blue continuum.

4.5.3. $MLS1519-13$ ($MLS110526:151937-130602$)

$MLS1519-13$ has a highly variable CRTS light curve between 18.5 and 19.6 mag. The SOAR spectrum resembles A or F spectral type, with narrow Balmer absorptions and blue continuum. The time-series analysis of the CRTS photometric data yielded a period of 0.521 d. The light curve of the CRTS data folded on this period shows a 1 mag amplitude modulation (Figure 5, top panel). The spectroscopic features and light curve shape indicate that $MLS1519-13$ is a RR Lyrae star.

4.5.4. $MLS2044-16$ ($MLS111021:204455-162230$)

The CRTS photometric measurements vary from 14.2 to 15.5 magnitudes and it matches a blue source in SDSS DR9. The H lines are visible in absorption in the spectrum while the continuum is blue. The time-series analysis of the CRTS photometric data yielded a period of 0.535 d. The light curve of the CRTS data folded on this period is presented in Figure 5 (middle panel). From its typical light curve and spectral features this source is classified as a RR Lyrae variable.

4.5.5. $MLS2132-15$ ($MLS100620:213227-150523$)

$MLS2132-15$ is another new RR Lyrae variable star. The CRTS light curve varies between 17 and

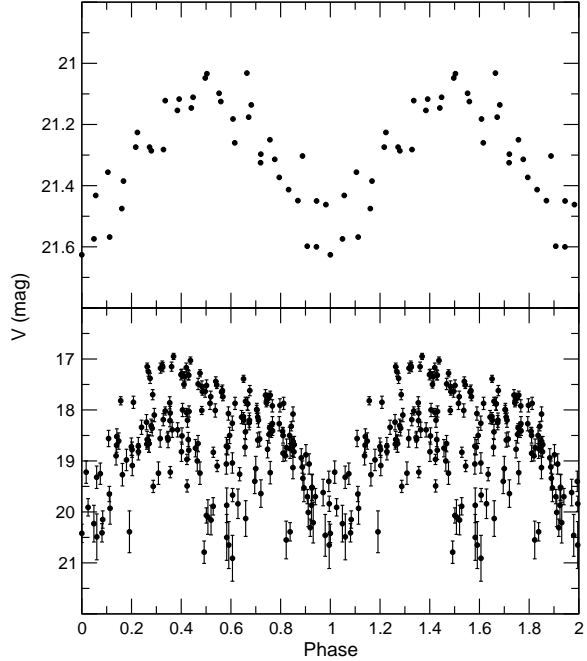


Fig. 4.— OPD (upper panel) and CRTS (lower panel) light curves of $MLS1519-13$, both folded

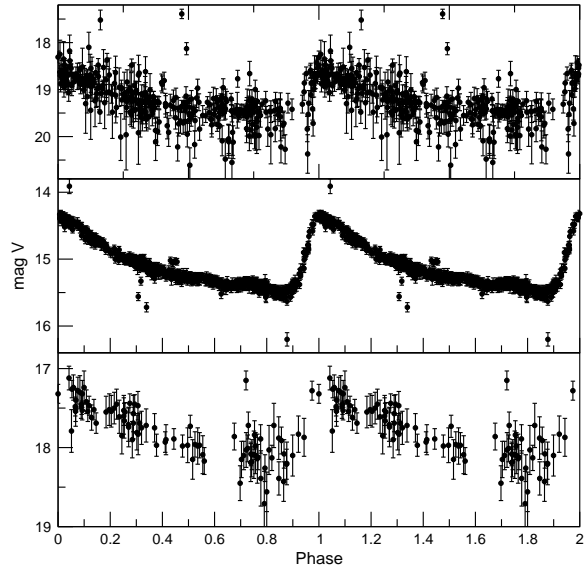


Fig. 5.— CRTS photometric data of $MLS1519-13$ (top), $MLS2044-16$ (middle) and $MLS2132-15$ (bottom) folded with the periods described in the respective sections.

18.5 mag, while our spectrum presents Balmer absorption features over a blue continuum. We found a period of 0.486 d from the CRTS data. The folded CRTS light curve is shown in the bottom panel of Figure 5.

4.6. Mira and Low-Amplitude Pulsating Red Giants Stars

Low and intermediate-mass pulsating red giants, located at the asymptotic giant branch, are classified as Mira, semi-regular (SR) or late type slow irregular (LB) variables in the General Catalogue of Variable Stars (GCVS, Kholopov et al. 1985). The classification in the GCVS is based only on the amplitude and periodicity of the visual variation. Miras have amplitudes above 2.5 magnitudes, reaching up to 10 mag, and are fairly regular with periods from 80 to 1000 days, while SRs show lower amplitudes, from hundredths of magnitudes to 2.5 mag. This 2.5 mag threshold, however, is arbitrary. The LB class encompasses slow irregular variables of late spectral classes with no evidence of (or poorly defined) periodicity.

4.6.1. *SSS1448-40 (SSS100507:144833-401052)*

The light curve of SSS1448-40 has an amplitude of 1 mag at an average magnitude of 12.4 mag. The exploratory spectrum presents TiO molecular bands and is well fitted by a M7-M8 III spectral type (Figure 6, top panel). From those photometric and spectroscopic features SSS1448-40 is possibly a SR variable. The DFT and Lomb-Scargle methods applied to the CRTS data gave a period of 87 ± 1 d. The phase diagram of the data folded with this period is shown in the upper panel of Figure 7.

4.6.2. *SSS1639-23 (SSS100804:163911-235804)*

The amplitude of the CRTS light curve of this object is 3 mag, with an average level at 14 magnitude. The spectrum is quite similar to the spectrum of the Mira type star R Leo (Figure 6, middle panel). The Mira classification is corroborated by the large amplitude of the optical variation, greater than 2.5 mag. The period search performed with DFT and Lomb-Scargle on the CRTS data yielded a period of 307 ± 16 d. The folded lightcurve can be seen in Figure 7 (lower panel).

4.6.3. *SSS1940-63 (SSS110625:194030-633056)*

This object has a low amplitude light curve (0.3 mag) at 15 average magnitude. The spectrum corresponds to M5 spectral type, but it is slightly better fitted as luminosity class V than III (Figure 6, bottom panel). The star is possibly another low-amplitude Pulsating Red Giant.

4.7. Extragalactic Objects

The seven sources described below were classified as extragalactic sources because of the redshift of the lines identified in their spectra. Five of them are dominated by broad Mg II 2798 Å lines and blends of Fe II multiplets in the UV region. These features are characteristics of active galactic nuclei (AGN), in addition to the large variability in virtually all wavebands. The remaining two objects display both emission and absorption lines, with strengths typically observed in galaxies with on-going stellar formation. No information on redshifts for none of these seven objects are available in the literature. We searched for counterparts in other catalogues such as GALEX, HST, ROSAT and NVSS to detect emission in other spectral regions. We found that most of the targets have been detected by GALEX, in accord to the information provided by the SOAR spectra. Thus, to the best of our knowledge, we provided here first classification and redshift of these sources.

4.7.1. *CSS0213+00 (CSS091215:021311+002153)*

This CRTS object varies between 20.5 and 18.5 mag and was suggested to be a polar type CV or an AGN⁷. The SOAR exploratory spectrum is compatible with an AGN at $z=1.257$ based on the conspicuous broad emission line of Mg II 2798 Å and numerous blended UV Fe II multiplets in the spectral region covered by our data. The presence of both permitted iron lines and a broad Mg II 2798 Å line allow us to classify this source as a Type I AGN. We measured the FWHM of the Mg II 2798 Å and found a value of 31 Å. Following Weymann et al. (1991), we use the rest-frame “W2400” equivalent width, defined between the two continuum windows 2240–2255 and 2665–2695 Å with the integration for the equivalent width between 2255–2650 Å as the index of UV Fe II emis-

⁷<http://nesssi.cacr.caltech.edu/catalina/Circulars/912151010124106434.htm>

sion. For CSS0213+00 we measured a W_{2400} index of 25 \AA , which classifies this source as an weak Fe II emitter. CSS0213+00 has several counterparts at SDSS within a radius of $0.5'$. The one that matches to the SOAR position is classified as a star by SDSS. There is, though, an extended source classified as a galaxy, offset by $0.25'$ from the SOAR position (SDSS J021311.67+002204.3) with $g = 20.65$, $r = 19.428$, compatible with the magnitudes derived from this work. Other candidate GALEX targets are at least 2 magnitudes fainter.

4.7.2. *CSS0315-01 (CSS071206:031525-014051)*

CSS0315-01 was discovered by CRTS in 2007 December 6 and shows a light curve slowly varying between 19 and 20.5 mag. Broad Mg II 2798 \AA and the UV Fe II multiplets are the two most prominent features in the observed spectrum. The presence of these two characteristics classifies CSS0315-01 as a Type I AGN. This classification is further confirmed due to the presence of [Ne V] 3425 \AA , a forbidden high-ionization line that is typical of AGNs. [O II] $\lambda\lambda 3727, 3729\text{ \AA}$ are also detected. The redshift we derived for this source is $z=0.8513$. There is a UV counterpart identified by GALEX (GALEXASC J031525.15-014039.8) very close in position to CSS0315-01 ($0.17'$ away), with a NUV GALEX AB magnitude of 20.07, in accord to the magnitude derived from optical observations.

4.7.3. *CSS1240-15 (CSS071218:124027-150558)*

This transient, discovered by CRTS, is highly variable in the range from 18.5 to 21 mag. The spectrum presents narrow emission lines of [O] II $3726/3728\text{ \AA}$, the brightest line present in the spectral interval covered by SOAR, H γ , H β and [O] III $4959/5007\text{ \AA}$ at a redshift $z = 0.272$. Besides, absorption lines of Ca II H and K are detected. An upper limit to the line flux ratio [O] III/H β derived for this source is 0.39. This value classifies CSS1240-15 as a H II galaxy (Kewley et al. 2006). Additional support to this classification comes from the line ratio [O] II/[O] III, for which we measured a value of 5.4 ± 0.6 (Baldwin et al. 1981). There is a UV counterpart identified by GALEX (GALEXASC J124027.56-150559.3) very close in position to CSS1240-15, offset by $0.14'$ with NUV (GALEX)

AB magnitude of 21.61 ± 0.28 , compatible with the minimum magnitude measured from variability. The large amplitude variability of this source is not compatible with the classification obtained from the SOAR spectroscopy. This is because H II galaxies are not known to be highly variable. Thus, it is very likely that CSS1240-15 is indeed an AGN caught at a minimum state, with the central source completely hidden from direct view. It is also possible that it is a low excitation radio AGN (LERAG, Padovani et al. 2015) although it is not detected in the NVSS survey. Follow-up spectroscopy is necessary to unveil the real nature of this object.

4.7.4. *MLS1251-02 (MLS110329:125118-020208)*

This source is highly variable in CRTS light curve, ranging from 16 to 22 mag in timescales of months. It is detected by SDSS (SDSS J125118.38-020207.5), with $u = 21.58$, $g = 21.35$, $r = 20.81$, $i = 20.57$ and $z = 20.05$ in DR9. The exploratory spectrum is quite peculiar. It corresponds to an AGN at $z=1.1887$, determined by the emission line at 6120 \AA , which we identify as Mg II 2798 \AA . Absorption doublets are clearly visible at 5700 \AA and 5010 \AA . These are Mg II $2796, 2803\text{ \AA}$ absorption-line systems from two distinct intervening gaseous clouds in the line of sight of the AGN, at redshifts of $z_1 = 1.037$ and $z_2 = 0.791$, respectively. The Mg II absorption system is a tracer of low-ionization and neutral gas and is frequently used to study the kinematics, ionization and chemical conditions of the clouds, considered to be low surface brightness galaxies, dwarf galaxies, halos of high surface brightness galaxies or remnant mass from galaxy formation (Churchill & Le Brun 1998; Quider et al. 2011). Other absorption features that are present in our spectrum are the doublet of Fe II $2586, 2600\text{ \AA}$, visible at 4640 \AA , and the Mg I 2852 \AA line, visible at 5108 \AA . Both are associated to the gaseous structure at $z_2 = 0.791$. The strong spectrophotometric variability of MLS1251-02 suggests that it is an optically violently variable (OVV) quasar. MLS1251-02 is also associated to a radio source detected by the NRAO VLA Sky Survey (NVSS) NVSS J125118-020207 (Healey et al. 2007) and to a GALEX source (GALEXASC J125118.43-020207.7). In the NVSS catalogue, it shows a flux of 127.9 ± 3.9 mJy at 1.4 GHz. This value

classifies it as a radio loud AGN. In the GALEX catalogue, two different NUV AB magnitudes are found: 20.91 ± 0.15 and 22.57 ± 0.21 , reflecting the strong variable of this object. MLS1251-02 is listed in NED as a QSO candidate. Thus, we confirm with our data the AGN nature of this object.

4.7.5. MLS1402-09 (MLS110301:140203-090329)

MLS1402-09 is a red source in SDSS ($u = 24.62$, $g = 22.79$, $r = 21.17$, $i = 20.44$ and $z = 19.89$) with a CRTS light curve displaying a low brightness level at 20.5 average magnitude and a high level at 19.5 – 20 mag. The spectrum shows a prominent narrow emission line at 5493 Å, which we identify as [O] II 3726/3728 Å. Absorption lines of Ca II H and K at 3934 Å and 3968 Å at laboratory wavelengths are also detected. From the observed position of [O] II, we derived a redshift of $z = 0.4736$. There is a GALEX UV source associated to this object (GALEXASC J140157.69-090333.1), with an integrated NUV (GALEX) AB magnitude of 21.84. In the NVSS catalog there is a radio source (NVSS J140203-090747) offset by $4.307'$ from MLS1402-09 with a measured flux of 3.2 ± 0.6 mJy at 1.4 GHz. This flux level classifies it as a low-emission radio AGNs (LERAG, Padovani et al. 2015). LERAG displays an optical spectrum typical of very low ionization sources but with a radio power at the level of AGN activity. This is very likely the case of MLS1402-09.

4.7.6. MLS1404-15 (MLS100617:140447-152226)

MLS1404-15 was suggested to be a CV by CRTS for its blue DSS color and high variability. The CRTS light curve has a low state at 19.5 average magnitude, changing to a high state at average 18.5 mag from 2009 on. The exploratory spectrum obtained with SOAR is outstanding. A prominent broad feature centered at 5321 Å, that we associated to Mg II 2798 Å at $z = 0.9017$ dominates the spectrum. We also identified the UV Fe II multiplets at both sides of Mg II 2798, typical of Type I AGNs. The presence of high-ionization lines of [Ne V] 3347,3427 Å and the permitted O III line at 3134 Å (at laboratory wavelength) give additional support that MLS1404-15 is indeed an AGN. A GALEX (GALEXASC J140446.91-152226.1) counterpart is coincident in position with MLS1404-15. Moreover, a ROSAT

X-ray source (1RXS J140445.1-152115) offset by $1.261'$ relative to the optical position listed in Table 1 is reported by Voges et al. (2000).

4.7.7. MLS2230-04 (MLS100906:223034-042347)

Classified as a possible variable star by CRTS, MLS2230-04 has a bimodal light curve with a low state at 20 mag and a high state at 19.3 mag. The SOAR spectrum is dominated by a broad Mg II 2798 Å emission line and hints of UV Fe II multiples at both sides of Mg II. Because of these two features, we classify this source as an Type I AGN at $z=0.968$. A GALEX source (GALEXASC J223033.59-042346.0) is within a search radius of $0.1'$ of MLS2230-04. It has a NUV (GALEX) AB magnitude of 22.11 ± 0.39 . This is significantly fainter than the magnitude derived from optical observations and may reflect the fact that MLS2230-04 is highly reddened or even more variable than expected, with the GALEX data taken at a minimum.

5. SUMMARY AND DISCUSSION

In this work we report a survey and a search of magnetic CVs based on an exploratory spectroscopy of objects selected from the CRTS light curves and also from the literature. Most of our measurements were carried out at SOAR telescope, but some objects were observed at OPD. From our initial sample of 47 objects, we found 32 sources which we classified as CVs based on the aspect of the exploratory spectra. This group is composed of 13 polars, 16 objects presenting quiescent disk, 2 objects in high-accretion state, and 1 nova. In addition to CVs, we have also found RR Lyrae stars, variable red giants and extragalactic objects. These results are summarized below.

We present spectra of 13 probable polars, being 5 of them new candidates. We present the first published spectrum for other 5 objects already suggested to be polars. In Ritter & Kolb (2003) catalogue (update RKcat7.23, 2015), there are 119 confirmed and 30 uncertain AM Her objects. Six objects of our sample are not included in RKcat7.23. Only 6 objects (out of 13) are known high-energy sources, which shows that the X-rays detection is not a *sine qua non* criterion for the classification as a polar (or a magnetic CV).

This is particularly true for faint/distant objects, which could be missed by soft X-rays surveys - see, for instance, the discussion of MLS0227+13 presented in Silva et al. (2015). Ten objects obey the two Silber (1992)'s criteria for mCV classification. The three remaining objects are peculiar in some way: 1RXS1002-19, which has emission lines too broad for a polar; CSS1127-05, which has the largest H β EW of our CV sample; and CSS1503-22, which presents absorption features in the H β region preventing a proper quantification of line indicators. Hence, Silber (1992)'s criteria seems to be adequate to define polars. MLS0227+13, an eclipsing polar, was previously studied by us using time-resolved photometry and polarimetry (Silva et al. 2015). We propose the orbital periods for MLS0456+18 ($P = 2.36$ h) and MLS1609-10 ($P = 1.85$ h).

We classify 16 objects as probable CV with quiescent disks. Many of those objects have the He II 4686 Å line and/or X-ray counterparts characteristic of mCVs, however these criteria are not enough to classify them as IPs, since dwarf novae can also present these features. Hence, it is more challenging to spectroscopically classify IPs compared to polars. Eventually, we suggest that 9 objects among those 16 CVs are possible IPs. From these 9 IP candidates, 8 are new suggestions and one (CTCV2056-30) was previously known as IP candidate. One of these 8 new suggested IPs is CSS0104-03. It has strong enough He II 4686 Å line to have its EW measured and, even in this case, its EW is smaller than 40% of H α EW, therefore too weak to obey the Silber (1992)'s criterion of a mCV. Even so, we classify it as a probable IP because its He II 4686 Å line is stronger in quiescence compared to brighter state.

The 7 remaining new IP candidates (namely CSS1012-18, SSS1359-39, MLS2043-19, MLS2054-19, CSS2200+03, SSS2242-66 and CSS2319+33) were classified as such by spectral similarity to CTCV2056-30. This object is a strong IP candidate due to its photometric variability modulated by the white dwarf rotation (Augusteijn et al. 2010). From these 7 objects, MLS2054-19 and CSS2200+03 were previously classified as CVs (but not as IPs). MLS2054-19 has a suggested photometric period of 0.09598 d. Assuming it is a SU UMa object, this variability was interpreted as a superhump period (Coppejans et al. 2014). In-

terestingly, if this is the orbital period, the object is in the period gap. CSS2200+03, on the other hand, had been previously classified as a polar, but it shows double peak lines indicating the presence of a disk. All of our nine IP candidates have He II 4686 Å in the spectra, 4 of them have X-ray counterparts and 8 have shown outbursts.

The spectrum of CTCV2056-30, whose orbital period is around 1.75 h, is very similar to the spectrum of several short-period IPs, like SDSS J2333, HT Cam and DW Cnc. While most of the polars have orbital periods below 4 h, few IPs have periods below the 2–3 h period gap. The Ritter & Kolb (2003) catalogue registers 68 confirmed IPs and only 9 of those have orbital periods below the gap. This may indicate that most of the IPs with longer periods evolve to short period polars, whereas those with lower magnetic fields remain as IPs (Norton et al. 2004). In order to understand the details of mCVs evolution, it is fundamental to have the sample of short period IPs as complete as possible. Follow-up studies of these candidates are essential, and may confirm their nature and help to build an homogeneous sample of IPs, which can be used to investigate the issue of mCV evolution.

Three remaining objects from our sample are CVs as well. Two of them have disks in high state of accretion: the known dwarf nova 1RXS0721-05, which we caught in eruption, and the newly discovered CV SSS2042-60, which we classify as a novalike, possibly of VY Scl type. We also confirmed that the transient high-energy source XMM0630-60 is a nova, which we observed in the nebular phase.

The confirmation of the classifications and the detailed nature of the CVs will be determined by time-resolved spectroscopic, photometric and polarimetric follow-up observations in the future.

From the rest of our sample of CRTS variable objects, 8 are pulsating stars. Our sample contains 5 RR Lyrae objects. Three of them are new discoveries and have pulsation periods around 0.5 d. We also discovered 3 new red variables, one of them being a Mira type star with a period of approximately 307 d.

We found 7 highly variable extragalactic objects with redshifts between $0.272 \leq z \leq 1.257$. Five of them (CSS0213+00, CSS0315-01, MLS1251-

02, MLS1404-15 and MLS2230-04) are compatible with an active galactic nucleus classification based on the presence of broad Mg II 2798 Å and UV Fe II multiplets. Previous GALEX/SDSS and/or NVSS detections of these objects give additional support to our classification. The remaining two sources (CSS1240-15 and MLS1402-09), also with detections in those catalogs, are most likely low excitation radio AGN. To the best of our knowledge, optical spectroscopy of these sources as well as their redshift or level of nuclear activity have never been published before.

We would like to thank J. E. Steiner for useful comments which helped to improve the paper. This study was partially supported by CNPq (CVR: 306701/2015-4 and 306103/2012-5, KMGS:302071/2013-0), FAPESP (LAA: 2012/09716-6 and 2013/18245-0; CVR: 2013/26258-4) and CAPES (MSP: 23038.009634/2016-71). This work is based partly on observations made at the Observatório do Pico dos Dias, Brazil, operated by the Laboratório Nacional de Astrofísica, and at the Southern Astrophysical Research (SOAR) telescope, which is a joint project of the Ministério da Ciência, Tecnologia e Inovação (MCTI) da República Federativa do Brasil, the US National Optical Astronomy Observatory (NOAO), the University of North Carolina at Chapel Hill (UNC) and Michigan State University (MSU). The CRTS survey is supported by the US National Science Foundation under grants AST-0909182. The CSS survey is funded by the National Aeronautics and Space Administration under grant no. NNG05GF22G issued through the Science Mission Directorate Near-Earth Objects Observations Program. STSDAS is a product of the Space Telescope Science Institute, which is operated by AURA for NASA.

REFERENCES

Afanasiev, V. L., Borisov, N. V., & Gabdeev, M. M. 2015, *AstBu*, 70, 328

Augusteijn, T., Tappert, C., Dall, T., & Maza, J. 2010, *MNRAS*, 405, 621

Baldwin, J. A., Phillips, M. M., & Terlevich, R. 1981, *PASP*, 93, 5

Beuermann, K., & Schwone, A. D. 1994, ASPC 56, *Interacting Binary Stars*, ed. A.W. Shafter (San Francisco, CA: ASP), 119

Beuermann, K., & Thomas, H.-C. 1993, *AdSpR*, 13, 115

Boller, T., Freyberg, M. J., Trümper, J., et al. 2016, *A&A*, 588, A103

Breedt, E., Gänsicke, B. T., Drake, A. J., et al. 2014, *MNRAS*, 443, 3174

Churchill, C. W., & Le Brun, V. 1998, *ApJ*, 499, 677

Clarke, D. 2002, *A&A*, 386, 763

Clemens, J. C., Crain, J. A., & Anderson, R. 2004, *Proc. SPIE*, 5492, 331

Coppejans, D. L., Körding, E. G., Knigge, C., et al. 2016, *MNRAS*, 456, 4441

Coppejans, D. L., Woudt, P. A., Warner, B., et al. 2014, *MNRAS*, 437, 510

Cowperthwaite, P. S., Massaro, F., D'Abrusco, R., et al. 2013, *AJ*, 146, 110

Cropper, M. 1990, *SSRv*, 54, 195

de Budè, D. L. 2011, Master of Science Thesis (Univ. of Cape Town)

Deeming, T. J. 1975, *Ap&SS*, 36, 137

Denisenko, D., & Martinelli, F. 2012, *PZ*, 32, 3

Denisenko, D. V., & Sokolovsky, K. V. 2011, *AstL*, 37, 91

Downes, R. A., Webbink, R. F., Shara, M. M., et al. 2001, *PASP*, 113, 764

Drake, A. J., Catelan, M., Djorgovski, S. G., et al. 2013, *ApJ*, 763, 32

Drake, A. J., Djorgovski, S. G., Mahabal, A., et al. 2009, *ApJ*, 696, 870

Drake, A. J., Gänsicke, B. T., Djorgovski, S. G., et al. 2014, *MNRAS*, 441, 1186

Drissen, L., Shara, M. M., Dopita, M., & Wickramasinghe, D. T. 1994, AJ, 107, 2172

Dworetsky, M. M. 1983, MNRAS, 203, 917

Fertig, D., Mukai, K., Nelson, T., & Cannizzo, J. K. 2011, PASP, 123, 1054

Gray, R. O., & Corbally, C., J. 2009, Stellar Spectral Classification (Princeton, NJ: Princeton Univ. Press)

Gunn, J. E., & Stryker, L. L. 1983, ApJS, 52, 121

Hamuy, M., Walker, A. R., Suntzeff, N. B., et al. 1992, PASP, 104, 533

Healey, S. E., Romani, R. W., Taylor, G. B., et al. 2007, ApJS, 171, 61

Hessman, F. V., Robinson, E. L., Nather, R. E., & Zhang, E.-H. 1984, ApJ, 286, 747

Hümmerich, S., Bernhard, K., & Srdoc, G. 2014, OEJV, 167, <http://var.astro.cz/oejv/oejv.php?lang=en>

Kann, D. A., Greiner, J., & Rau, A. 2011, ATel. 3813, <http://www.astronomerstelegram.org/?read=3813>

Kato, T., Hambach, F.-J., Maehara, H., et al. 2013, PASJ, 65, 23

Kemp, J., Patterson, J., Thorstensen, J. R., et al. 2002, PASP, 114, 623

Kewley, L. J., Groves, B., Kauffmann, G., & Heckman, T. 2006, MNRAS, 372, 961

Kholopov, P. N., Samus, N. N., Durlevich, O. V., et al. 1992, General Catalogue of Variable Stars, 4rd ed., vol.IV, Bull. Inf. CDS, 40, 15

Kryachko, T., Samokhvalov, A., & Satovskiy, B. 2010, IBVS 5952, <http://www.konkoly.hu/cgi-bin/IBVS?5952>

Lomb, N. R. 1976, Ap&SS, 39, 447

Mennickent, R. E., Tovmassian, G., Zharikov, S. V., et al. 2002, A&A, 383, 933

Mortier, A., Faria, J. P., Correia, C. M., Santerne, A., & Santos, N. C. 2015, A&A, 573, A101

Norton, A. J., Wynn, G. A., & Somerscales, R. V. 2004, ApJ, 614, 349

Ohshima, T. 2013, vsnet-alert 16294, <http://ooruri.kusastro.kyoto-u.ac.jp/mailarchive/vsnet-16294>

Padovani, P., Bonzini, M., Kellermann, K. I., Miller, N., Mainieri, V., Tozzi, P. 2015, MNRAS, 452, 1263

Patterson, J., Thorstensen, J. R., Vanmunster, T., et al. 2004, PASP, 116, 516

Pojmanski, G. 2002, AcA, 52, 397

Quider, A. M., Nestor, D. B., Turnshek, D. A., et al. 2011, AJ, 141, 137

Ramsay, G., & Cropper, M. 2003, MNRAS, 338, 219

Read, A. M., Saxton, R. D., & Esquej, P. 2011a, ATel. 3811, <http://www.astronomerstelegram.org/?read=3811>

Read, A. M., Saxton, R. D., & Esquej, P. 2011b, ATel. 3821, <http://www.astronomerstelegram.org/?read=3821>

Ritter, H., & Kolb, U. 2003, A&A, 404, 301 (update RKcat7.23, 2015)

Rodríguez-Gil, P., Gänsicke, B. T., Araujo-Betancor, S., & Casares, J. 2004, MNRAS, 349, 367

Saxton, R. D., Read, A. M., Esquej, P., et al. 2008, A&A, 480, 611

Scargle, J. D. 1982, ApJ, 263, 835

Schmidt, G. D., Szkody, P., Vanlandingham, K. M., et al. 2005, ApJ, 630, 1037

Schweppe, A. D., & Thinius, B. 2012, AN, 333, 717

Silber, A. D. 1992, Ph.D. Thesis (MIT)

Silva, K. M. G., Rodrigues, C. V., Oliveira, A. S., et al. 2015, MNRAS, 451, 4183

Southworth, J., Gänsicke, B. T., Marsh, T. R., de Martino, D., & Aungwerojwit, A. 2007, MNRAS, 378, 635

Stellingwerf, R. F. 1978, ApJ, 224, 953

Szkody, P., Anderson, S. F., Brooks, K., et al. 2011, AJ, 142, 181

Szkody, P., Everett, M. E., Howell, S. B., et al. 2014, AJ, 148, 63

Szkody, P., Henden, A., Fraser, O. J., et al. 2005, AJ, 129, 2386

Thorstensen, J. R., & Skinner, J. N. 2012, AJ, 144, 81

Voges, W., Aschenbach, B., Boller, T., et al. 2000, VizieR Online Data Catalog, <http://www.xray.mpe.mpg.de/rosat/survey/ra>

Warner, B. 1995, Cataclysmic Variable Stars (1st ed.; Cambridge, GB: CUP)

Weymann, R. J., Morris, S. L., Foltz, C. B., & Hewett, P. C. 1991, ApJ, 373, 23

Woudt, P. A., Warner, B., de Budé, D., et al. 2012, MNRAS, 421, 2414

York, D. G., Adelman, J., Anderson, J. E., Jr., et al. 2000, AJ, 120, 1579

Zacharias, N., Monet, D. G., Levine, S. E., et al. 2004, BAAS, 36, 1418

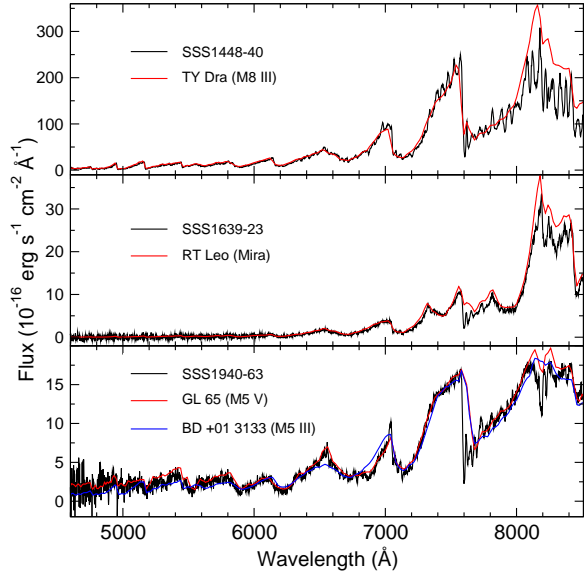


Fig. 6.— Spectra of SSS1448-40 (top), SSS1639-23 (middle) and SSS1940-63 (bottom). The black lines are our spectra and the red and blue lines are the fitted reference spectra used for the spectral type estimation, from the Bruzual-Persson-Gunn-Stryker Atlas (Gunn & Stryker 1983).

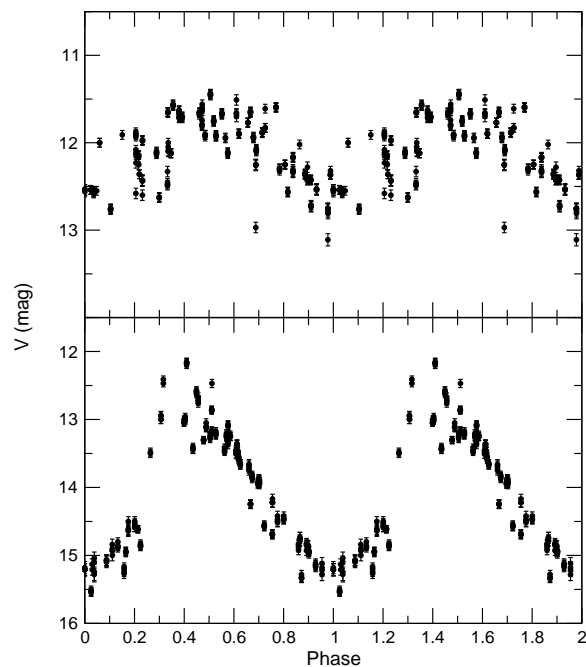


Fig. 7.— CRTS photometric light curves of SSS1448-40 (top) and SSS1639-23 (bottom) folded with periods of 87 d and 307 d, respectively - see text.